EUROPEAN ORGANIZATION FOR NUCLEAR RESEARCH

CERN-PPE/92-110
18 June 1992

A MEASUREMENT OF THE DECAY $K_L \to \pi^0\gamma\gamma$

G.D. Barr, P. Buchholz, R. Carosi, D. Coward[1,2], D. Cundy, N. Doble, L. Gatignon, P. Grafström, R. Hagelberg, H.N. Nelson[3] and H. Wahl
CERN, Geneva, Switzerland.

K. J. Peach
Physics Department, University of Edinburgh, Edinburgh, UK.

H. Blümer, R. Heinz, K. Kleinknecht, P. Mayer, B. Panzer[4] B. Renk, H. Rohrer and A. Wagner
Institut für Physik, Universität Mainz, Mainz, Germany[5]

E. Augé, D. Fournier[4], L. Iconomidou-Fayard, I. Harrus[6] O. Perdereau, A. C. Schaffer and L. Serin
Laboratoire de l'Accélérateur Linéaire, IN2P3-CNRS, Université Paris-Sud, Orsay, France[7]

L. Bertanza, A. Bigi, P. Calafiura[8] M. Calvetti[9] R. Casali, I.G. Mannelli[8], V.M. Marzulli[8], A. Nappi and G. Pierazzini
Dipartimento di Fisica e Sezione INFN di Pisa, Pisa, Italy.

M. Holder, A. Kreutz, M. Rost and R. Werthenbach
Fachbereich Physik, Universität Siegen, Siegen, Germany[10]

Submitted to Physics Letters

---

1) On leave from SLAC, Stanford, Calif., USA.
2) Work supported in part by the US Department of Energy contract DE-AC03-76F00515.
3) Present address: University of California, Santa Barbara, Calif., USA.
4) Present address: CERN, Geneva, Switzerland.
5) Funded by the German Federal Minister for Research and Technology (BMFT) under contract 054Mz18.
6) Present address: Columbia University, New York, New York, USA.
7) Funded by Institut National de Physique des Particules et de Physique Nucléaire (IN2P3), France.
8) Present address: Scuola Normale Superiore, Pisa, Italy.
9) Present address: Dipartimento di Fisica e Sezione INFN, Perugia, Italy.
10) Funded by the German Federal Minister for Research and Technology (BMFT) under contract 054Si74.

ABSTRACT

The full data set of the experiment NA31 at CERN has been used to analyse the decay mode $K_L \to \pi^0\gamma\gamma$. A signal of 63 events has been observed with an estimated background of 6.0 ± 1.7 events, corresponding to a branching ratio of $(1.7 \pm 0.3) \times 10^{-6}$ consistent with our previous result based on partial statistics. The invariant mass spectrum of the two photons is found to be consistent with chiral perturbation theory, and the decay is dominated by the $J = 0$ two-photon state.

1. INTRODUCTION

The decay $K_L \to \pi^0\gamma\gamma$ is of considerable theoretical interest. Firstly, it may be used to estimate the CP conserving contribution to the decay $K_L \to \pi^0 e^+e^-$ [1–3] via two-photon intermediate states. Such processes, with two virtual photons in a $J = 0$ state, are strongly helicity suppressed. This is not the case for the processes with the two photons in the $J = 2$ state. If both contributions are small enough, then the decay $K_L \to \pi^0 e^+e^-$ is dominated by CP violating contributions. In this paper, we present a measurement of the dominant $J = 0$, and a limit on the $J = 2$ two-photon contribution to the $K_L \to \pi^0\gamma\gamma$ decay.

Secondly, the decay $K_L \to \pi^0\gamma\gamma$ may be used to test the chiral perturbation theory, and some semi-empirical models describing kaon decays. Lowest order chiral expansion [4] and models involving $\pi^+\pi^-$ intermediate states in addition to the π^0 [5] predict a branching ratio around 7×10^{-7} and $J = 0$ for the photon pair. The $\gamma\gamma$ invariant mass spectrum extends from about $2m_\pi$ to the kinematical limit. Higher order chiral expansion and other calculations including vector (or scalar) meson intermediate states [6] predict a branching ratio between 0.7×10^{-6} and 3×10^{-6} depending on the contribution at low $m_{\gamma\gamma}$, for which the photon pair should have $J = 2$.

We report here on a new analysis of the full data set collected with the NA31 detector in the years 1986, 1988, and 1989, which corresponds to more than twice the K_L flux that was used for our first observation [7] of this decay.

2. EXPERIMENTAL SET-UP AND DATA TAKING

The experiment was set up at the CERN SPS primarily to measure the parameter ϵ'/ϵ which characterizes direct CP violation in neutral kaon decays into two pions. This measurement was done by comparing the K_L and K_S decay rates into $\pi^0\pi^0$ and $\pi^+\pi^-$ final states [8]. The $K_L \to \pi^0\gamma\gamma$ final states appear nearly identical to the $\pi^0\pi^0$ ones in all the detector elements. The $K_L \to \pi^0\gamma\gamma$ branching ratio is obtained from the ratio of the number of observed $\pi^0\gamma\gamma$ events to the number of $\pi^0\pi^0$ ones with acceptance corrections determined by Monte Carlo simulation.

The beam and detector for the experiment have been described in detail in Ref. [9]. Long-lived kaons are produced with an average momentum of 100 GeV/c by 450 GeV/c protons striking a beryllium target located 244 m upstream of the electromagnetic calorimeter. Charged particles are removed by a sweeping magnet, and a neutral beam is selected by collimation to ± 0.2 mrad. The final collimator, with a diameter of 6 cm, is located 124 m upstream of the electromagnetic calorimeter. It is followed by a 95 m long evacuated region. The neutral beam is further transported in an evacuated tube of 20 cm diameter through a central hole in the detectors. Decays occurring in the upstream part of the evacuated region are measured. The outer diameter of the detectors is typically 2.5 m. The details of the detectors relevant for the present study are summarized below:

i) A liquid-argon/lead sandwich calorimeter with 1.25 cm wide strips read out in x and y projections transverse to the beam, and separated into quadrants. For photons, the energy resolution is $7.5\%/\sqrt{E(\mathrm{GeV})}$ and the position resolution is 0.5 mm in each projection.

ii) A scintillator hodoscope inside the liquid-argon calorimeter used for triggering on electromagnetic activity.

iii) Four ring-shaped anticounters surrounding the decay region, and placed between 60

and 120 m from the final collimator, to veto events with photons missing the calorimeter.

iv) Two wire chambers 23 m apart (25 m in 1986) to veto events with charged particles.

v) An iron/scintillator sandwich calorimeter to veto final states with hadronic energy.

3. EVENT SELECTION AND ANALYSIS

The relevant trigger requires a minimum total energy of 35 GeV, with at least two and at most four energy clusters in both transverse projections in the liquid-argon calorimeter. Events with photons or muons detected by the anticounters are rejected. Loose requirements are made on the decay position of purely electromagnetic final states, under the assumption that the decaying particle has the kaon mass. The trigger makes no requirement on the invariant mass of pairs of showers.

The raw data sample consists of 5×10^8 events. Showers in the liquid-argon calorimeter are reconstructed by the same program as used for the $K_L \to 2\pi^0 \to 4\gamma$ analysis of ϵ'/ϵ [8]. The program is able to recognize photons with energies above 2.5 GeV with good efficiency. The $K_L \to \pi^0\gamma\gamma$ candidates have to meet the following requirements:

i) They must have exactly four reconstructed electromagnetic showers. Each of these showers has an energy between 5 and 100 GeV, a distance > 16 cm from the beam axis, and a distance > 2.5 cm from the border lines separating the calorimeter into quadrants. All showers are separated by at least 5 cm in the x and y projections.

ii) The total energy of an event must be between 60 and 170 GeV.

iii) The events have no space points in the upstream wire chamber, but may have one space point in the downstream wire chamber to allow for backsplash from the calorimeter.

iv) The energy seen in the hadron calorimeter is less than 3 GeV.

v) The energy barycentre in the electromagnetic calorimeter is within 5 cm from the beam axis. Events with large missing transverse energy are rejected by this cut.

The longitudinal position Z_K of the decay vertex, as measured from the downstream face of the final beam collimator, is calculated from the energy and position of the four showers under the assumption that the invariant mass is the nominal kaon mass. For K^0 decays with undetected decay particles, Z_K is shifted towards the calorimeter with respect to the true vertex position. We therefore require Z_K to lie in the first 20 m downstream of the final collimator.

The four showers are grouped in two pairs. One pair is required to have a mass near the nominal π^0 mass, assuming a decay at Z_K, but no pairing should resemble a $\pi^0\pi^0$ final state. The $\gamma\gamma$ mass resolution for a π^0 is 1.8 MeV/c^2. The $\pi^0\gamma\gamma$ candidates are required to have a pair of showers, labelled (12) with invariant mass m_{12} between 125 and 145 MeV/c^2 (and closest to 135 MeV/c^2). The other pair is labelled (34).

The quantity μ defined below allows rejection of the $\pi^0\pi^0$ final states:

$$\mu = \left(\frac{m_{ij} - m_{kl}}{12\ \mathrm{MeV}/c^2}\right)^2 + \left(\frac{m_{ij} + m_{kl} - 2m_\pi}{8\ \mathrm{MeV}/c^2}\right)^2 ,$$

where m_{ij} and m_{kl} are the invariant masses of any two $\gamma\gamma$ pair combinations.

The $K_L \to \pi^0\gamma\gamma$ candidates are required to have μ above 5 for all possible pairings of the four showers. Using the available K_S data, and assuming that all four shower candidates are indeed $K_S \to \pi^0\pi^0$ decays, we estimate that the cut on μ rejects 99.8% of the selected $\pi^0\pi^0$ events. Seventy per cent of the $\pi^0\pi^0$ events remaining after the μ cut

are further rejected by removing events with two photons of comparable energies in the same quadrant of the calorimeter. Owing to the projective readout, there is in such a case a twofold ambiguity for combinations of the clusters in x and y projections, which may result in badly reconstructed events.

A total of 5881 $K_L \to \pi^0\gamma\gamma$ candidates survive the preceding selection. The majority of these events are background from $K_L \to 3\pi^0$ decay. The loss of photons that miss the detectors, as well as overlap of showers in the calorimeter, can result in the reconstruction of only four showers. A Monte Carlo simulation of a large number of $K_L \to 3\pi^0$ decays was used to devise additional cuts on the showers and requirements based on the event kinematics. These cuts strongly reduce the background.

A sample of 9×10^8 $K_L \to 3\pi^0$ decays was simulated. The true position of the vertex was generated between 18 m upstream of the final collimator and 28 m downstream. The propagation of these events through the collimators and detectors was fully simulated, and they were reconstructed in the same way as real data. The sample surviving the cuts described above has the following properties:

i) Approximately 60% of the sample results from the loss of two photons that miss the detector. Most of these events correspond to decays just upstream of the collimator, and at least one photon is lost in the collimator walls. The reconstructed vertex Z_K is shifted downstream by at least 7.5 m with respect to the true vertex.

ii) The other 40% of the sample results from one photon missing the detector and two showers overlapping in the electromagnetic calorimeter. As in (i), the reconstructed vertex is shifted by at least 7.5 m with respect to the true vertex. Moreover, one of the reconstructed showers is broader than for a single isolated photon.

iii) One per cent of the events have all six photons hitting the calorimeter, but only four showers reconstructed because of overlap. One or two showers are broader than for a single isolated photon.

If the distance between two photons is more than 1.5 cm in one projection, then the two showers can be resolved. When they overlap in a projection, the width of the merged energy clusters is larger than for a single photon. We define the quantity C to be the r.m.s. width of the energy distribution in a cluster's five central readout strips. The quantity C^* is the maximum of the r.m.s. widths of each of the two projections of each of the four showers. Its distribution is shown in Fig. 1 for simulated $K_L \to 3\pi^0$ and $K_L \to \pi^0\gamma\gamma$ events. Real $K_S \to 2\pi^0$ events are also shown. We reject events with $C^* > 1.1$ cm.

A second form of overlap is due to the projective readout of the calorimeter. A photon shower can overlap a second photon shower in the x projection, and simultaneously overlap a third photon shower in the y projection. If this happens, the energy of the x and y clusters, E_x and E_y are in general unequal. For each shower, we therefore require the energy asymmetry $A = (E_x - E_y)/(E_x + E_y)$ to be zero within three standard deviations.

A total of 3169 $\pi^0\gamma\gamma$ candidates remain after these cuts. The distribution of the reconstructed decay vertex Z_K for these events is displayed in Fig. 2. It rises steeply with increasing Z_K and more than 80% of the events are above $Z_K = 15$ m, in good agreement with what is expected from $3\pi^0$ background events. On the contrary, one expects a flat distribution for $\pi^0\gamma\gamma$ events.

The simulation described above shows that the true decay vertex for the remaining $3\pi^0$ background events is localized around the final collimator. To estimate the true vertex position for these events, we classify them in three categories (see Fig. 3):

a) any two of the six photons miss the detector;

b) one of the six photons misses the detector, and its partner from the same π^0 overlaps with another photon;

c) one of the six photons misses the detector, its partner from the same π^0 is correctly measured, and two photons from the other π^0's overlap.

Categories (a) and (b) contain at least one reconstructible π^0. For each pair of showers — there are five combinations other than (12) — the longitudinal position of the vertex is computed from the two shower energies and positions, assuming the invariant mass to be the nominal π^0 mass. If one of the five combinations gives a decay vertex in the region where $3\pi^0$ decays are expected, the event is rejected. As explained before, the upper limit of this region is $Z_{\rm K} - 7.5$ m. The lower limit is -15 m for $Z_{\rm K} > 10$ m, and $-(Z_{\rm K} + 5$ m) for $Z_{\rm K} < 10$ m. We denote by Z_π the vertex estimate which is closest to and smaller than $Z_{\rm K} - 7.5$ m.

To eliminate events from category (c), we reconstruct the common decay vertex of the two π^0's which give three showers. Let E_1, E_2, E_3 denote the shower energies, and d_{12}, d_{23} the distances between the showers in the calorimeter. Assuming two π^0's, the common decay vertex is given by

$$Z = 124 \text{ m} - \frac{1}{m_\pi} \times \left(\frac{1}{E_1 E_2 d_{12}^2} + \frac{1}{E_2 E_3 d_{23}^2} \right)^{-1/2} ,$$

where the distance from the final collimator to the calorimeter is 124 m, and $m_\pi = 135$ MeV/c^2.

Moreover, under the above assumptions, the invariant mass of the three showers cannot exceed $m_{\rm K} - m_\pi$. If any of the twelve triplets of the four showers has an invariant mass below $m_{\rm K} - m_\pi$ and gives a measurement of the common vertex in the same region as for categories (a) and (b), the event is rejected. We denote by $Z_{\pi\pi}$ the vertex estimate which is closest to and smaller than $Z_{\rm K} - 7.5$ m. For each event, we also have $Z_{\rm max} = \max(Z_\pi, Z_{\pi\pi})$.

According to the Monte Carlo simulation, the preceding two requirements reject 99.6% of the remaining $3\pi^0$ background, while 54% of the remaining $\pi^0\gamma\gamma$ signal is lost. More than half of the residual $2\pi^0$ background is also eliminated. In Fig. 4a, $Z_{\rm max}$ is plotted against $Z_{\rm K}$ for simulated $\pi^0\gamma\gamma$ events. Figures 4b and c show the same distribution for simulated $3\pi^0$ events and for real $\pi^0\gamma\gamma$ candidates.

Ninety-four candidates remain after all cuts. Figure 5 shows a significant peak in the m_{12} distribution at the π^0 mass. We define the signal region as the mass interval from 132.5 to 137.5 MeV/c^2. It corresponds to ± 1.4 times the r.m.s. resolution. Sixty-three events are in this region.

Both the $2\pi^0$ and the $3\pi^0$ simulations indicate that the residual background may be estimated by linear interpolation in the signal region from side bands (125 to 130 MeV/c^2 and 140 to 145 MeV/c^2). These side bands contain 12 events, whereas 6 events were expected from the simulations. From the number of observed side-band events, we estimate the residual background in the signal region to be 6.0 ± 1.7 events and conclude that we have observed 57 ± 8.1 $\rm K_L \to \pi^0\gamma\gamma$ decays within our cuts.

The distribution of the decay vertex $Z_{\rm K}$ for the 63 events in the signal region is shown in Fig. 6. It is in agreement with the $\rm K_L \to \pi^0\gamma\gamma$ simulation. In particular, there is no evidence for a shift towards large $Z_{\rm K}$ that would result from unobserved decay particles.

4. BRANCHING RATIO AND CHARACTERISTICS OF THE SIGNAL

To measure the branching ratio, we normalize our 57 events to the corresponding $K_L \to 2\pi^0$ events within identical cuts (except the μ cut) in order to minimize the uncertainty in the acceptance corrections. The ratio of acceptances for $\pi^0\gamma\gamma$ and for $\pi^0\pi^0$ is calculated to be 0.72 ± 0.02. It varies by ± 0.05 when the parameter a_V (which characterizes the contribution from the intermediate vector mesons in the notations of Ref. [4]) varies from -1.5 to $+1.5$.

The number of observed $K_L \to 2\pi^0$ events is $(4.24 \pm 0.02) \times 10^4$. Using the $K_L \to 2\pi^0$ branching ratio from Ref. [10], we obtain

$$\frac{\Gamma(K_L \to \pi^0\gamma\gamma)}{\Gamma(K_L \to \text{all})} = (1.7 \pm 0.2) \times 10^{-6} ,$$

where the error is purely statistical. We estimate the systematic uncertainty to be $\pm 0.2 \times 10^{-6}$, determined by the residual background estimate, the acceptance correction, the energy scale, and the experimental $K_L \to 2\pi^0$ branching ratio used.

The above branching ratio is slightly higher than the predictions of chiral perturbation theory to lowest order [4]. It agrees better with more elaborate estimates which include vector-meson contributions, together with other higher order terms in the chiral expansion [6]. It is consistent with our first result [7] (with or without a cut on m_{34} at 280 MeV/c^2), with a precision that is better by a factor of 2. It is also consistent with the result from the E731 Collaboration at FNAL [12].

In order to investigate the decay mechanism of the observed process, we study the distribution of the events in the invariant mass of the photon pair m_{34} and in the other Dalitz plot variable $y = |E_3 - E_4|/m_K$, calculated in the kaon rest frame. Events with two possible pairings giving m_{12} in the 130–140 MeV/c^2 mass range are excluded from this plot in order to avoid events which have an ambiguous assignment for m_{34}. Figures 7a and b show m_{34} and y for the 50 unambiguous events. The data show that the signal is dominantly at high m_{34} (above 240 MeV/c^2) as predicted by chiral models or models involving 2π intermediate states producing two photons with $J = 0$. There are only three events with m_{34} below 240 MeV/c^2, with an expected background of 1.5 events. There is no evidence for a signal below 240 MeV/c^2.

Taking into account the variation of the detector acceptance with m_{34}, we calculate the limit

$$\frac{\Gamma(m_{34} < 240 \text{ MeV}/c^2)}{\Gamma(\text{all } m_{34})} < 0.09 \quad (90\% \text{ CL}) .$$

This result translates into limits on a_V. According to the simulation, we obtain

$$-0.38 < a_V < 0.41 \quad (90\% \text{ CL}) .$$

Refining this analysis, we performed a maximum likelihood fit of a_V to the total data set as a function of the two Dalitz plot variables m_{34} and y. The result is :

$$a_V = -0.05^{+0.14}_{-0.17} ,$$

which may be translated into a 90% confidence level limit of $-0.32 < a_V < +0.19$.

The observed rate of $K_L \to \pi^0\gamma\gamma$ decays combined with this limit leads to the prediction [4] that the CP conserving contribution to the decay $K_L \to \pi^0 e^+ e^-$ has a branching ratio smaller than 4.5×10^{-13} (90% CL).

5. CONCLUSION

The measured branching ratio for the decay $K_L \to \pi^0\gamma\gamma$ is in good agreement with expectations from chiral perturbation theory. This includes models with and without contributions from intermediate vector mesons. However, the invariant mass distribution of the two photons strongly favours models involving chiral perturbation theory with a dominant contribution from the $J = 0$ two-photon system. This agreement and the smallness of a_V give further confidence in the estimates [12] showing that the CP conserving contribution to the $K_L \to \pi^0 e^+ e^-$ decay is small compared with the CP violating contributions.

Acknowledgements

We thank E. De Rafael, G. Ecker, L. Sehgal and A. Pich for their continuing interest in this measurement and for very valuable discussions on the interpretation of the result. We acknowledge the work done by M.C. Carrozza, C. Cerri, R. Fantechi, A. Giacomucci, V. Gibson and H.G. Sander. We express our gratitude to all the technical collaborators from the participating institutions and affiliated computing centres for their continuous efforts in the operation of the experiment and in the processing of the data. We are especially indebted to G. Kesseler and J. Van der Lans and their team.

REFERENCES

[1] J.F. Donoghue, B.R. Holstein and G. Valencia, Phys. Rev. **D35** (1987) 2769.
C.O. Dib, I. Dunietz, F.J. Gilman, Phys. Rev. **D39** (1989) 2639 and references therein.

[2] A. Barker et al., Phys. Rev. **D61** (1990) 3546.

[3] K.E. Ohl el al., Phys. Rev. Lett. **64** (1990) 2755.

[4] G. Ecker, A. Pich and E. De Rafael, Phys. Lett.**B189** (1987) 363.

[5] L.M. Sehgal, Phys. Rev. **D6** (1972) 367.
P. Ko and J.L. Rosner, Phys. Rev. **D40** (1989) 3775.

[6] G.W. Intemann, Phys. Rev. **D13** (1976) 654.
L.M. Sehgal, Phys. Rev. **D38** (1988) 808.
T. Morozumi and H. Iwasaki, Prog. Theor. Phys. **82** (1989) 371.
J. Flynn and L. Randall, Phys. Lett. **B216** (1989) 221.
G. Ecker, A. Pich and E. De Rafael, Phys. Lett. **B237** (1990) 481.
L.M. Sehgal, Phys. Rev. **D41** (1990) 161.
M.K. Volkov, Yad. Fiz. **53** (1991) 764.
J. Bijnens, S. Dawson and G. Valencia, Phys. Rev. **D44** (1991) 3555.

[7] G.D. Barr et al., Phys. Lett. **B242** (1990) 523.

[8] H. Burkhardt et al., Phys. Lett. **B206** (1988) 169.
H. Burkhardt et al., Phys.Lett. **B199** (1987) 139.

[9] H. Burkhardt et al., Nucl. Instrum. Methods **A268** (1988) 116.

[10] Particle Data Group, G. Yost et al., Phys. Lett. **B239** (1990) 1.

[11] G. Ecker et al., Nucl. Phys. **B303** (1988) 665.

[12] V. Papadimitriou et al., Phys. Rev. **D44** (1991) 573.

Figure captions

Fig. 1: Maximum cluster width C^* of the showers in the electromagnetic calorimeter, for simulated $K_L \to \pi^0\gamma\gamma$ events (solid), simulated $K_L \to 3\pi^0$ events (dashed), and real $K_S \to 2\pi^0$ events (dotted)

Fig. 2: Reconstructed kaon decay vertex Z_K for $K_L \to \pi^0\gamma\gamma$ candidates (points) and for simulated $K_L \to 3\pi^0$ background (dotted line). The simulation is normalized to the K_L flux, as determined from the $K_L \to 3\pi^0$ events accepted by the trigger.

Fig. 3: Topology of background categories for $K_L \to 3\pi^0$ decays with four reconstructed showers.

Fig. 4: Best estimate of the decay vertex under the $K_L \to 3\pi^0$ hypothesis (Z_{max}) as a function of the estimate of the decay vertex under the $K_L \to 4\gamma$ hypothesis (Z_K): (a) for simulated $K_L \to \pi^0\gamma\gamma$, (b) for simulated $K_L \to 3\pi^0$, and (c) for real $K_L \to \pi^0\gamma\gamma$ candidates. Events above the line are rejected.

Fig. 5: Invariant mass m_{12} for $K_L \to \pi^0\gamma\gamma$ candidates (solid) and for expected background from $2\pi^0$ and $3\pi^0$ simulations (dotted). The Gaussian represents the expected resolution.

Fig. 6: Distribution in the decay vertex position Z_K for $K_L \to \pi^0\gamma\gamma$ candidates with m_{12} in the signal region (solid), for candidates with m_{12} in the side bands, properly normalized (dashed), and for $K_L \to \pi^0\gamma\gamma$ events simulated with $a_V = 0$ (dotted).

Fig. 7a: Invariant mass m_{34} distribution for unambiguous $K_L \to \pi^0\gamma\gamma$ candidates with m_{12} in the signal region (solid), in the side bands properly normalized (dashed), and for $K_L \to \pi^0\gamma\gamma$ events simulated with $a_V = 0$ (dotted). The acceptance is given by the crosses.

Fig. 7b: Distribution of the Dalitz-plot y variable for $K_L \to \pi^0\gamma\gamma$ candidates with m_{12} in the signal region (solid), in the side bands (dashed) properly normalized, and for $K_L \to \pi^0\gamma\gamma$ events simulated with $a_V = 0$ (dotted).

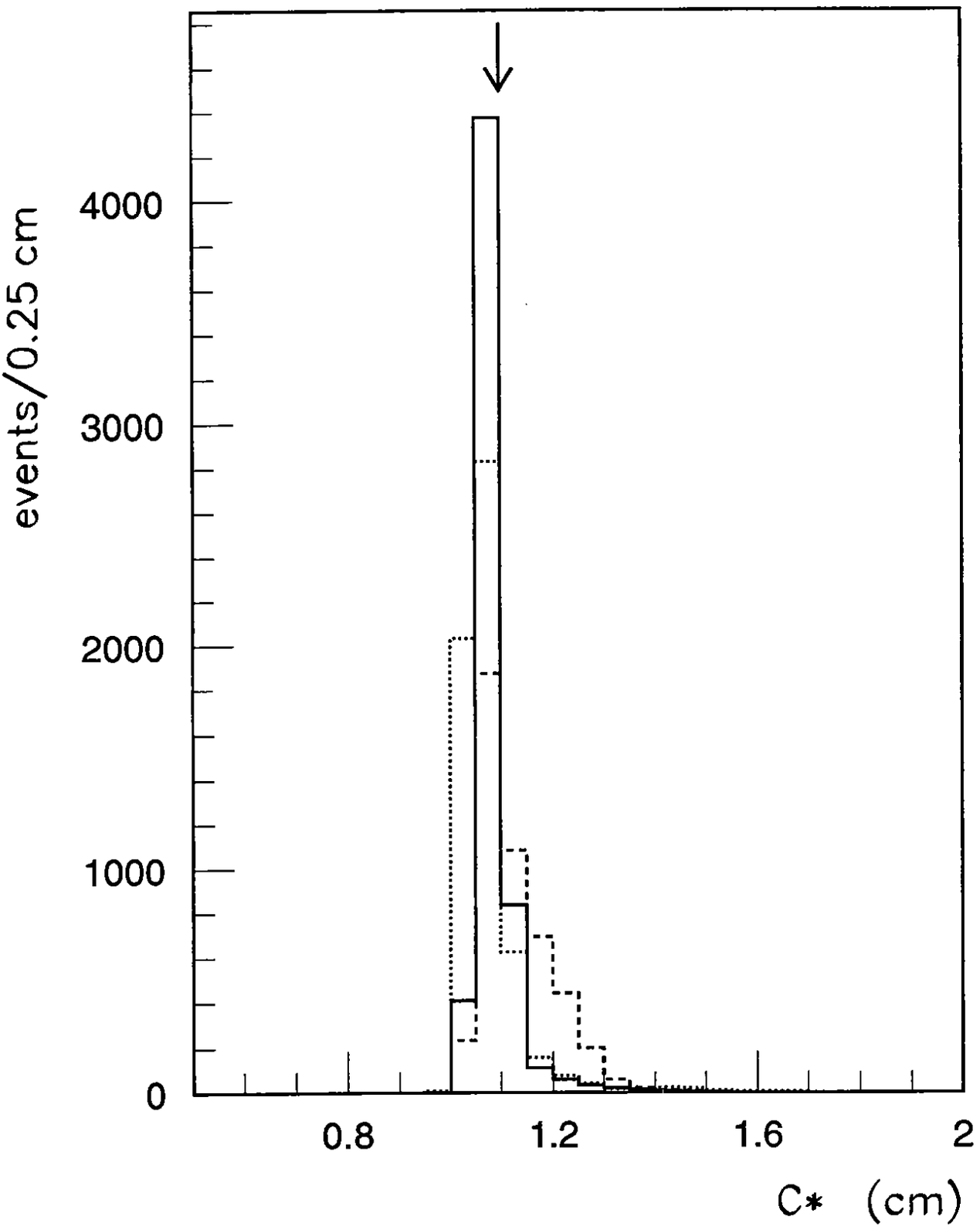

Figure 1

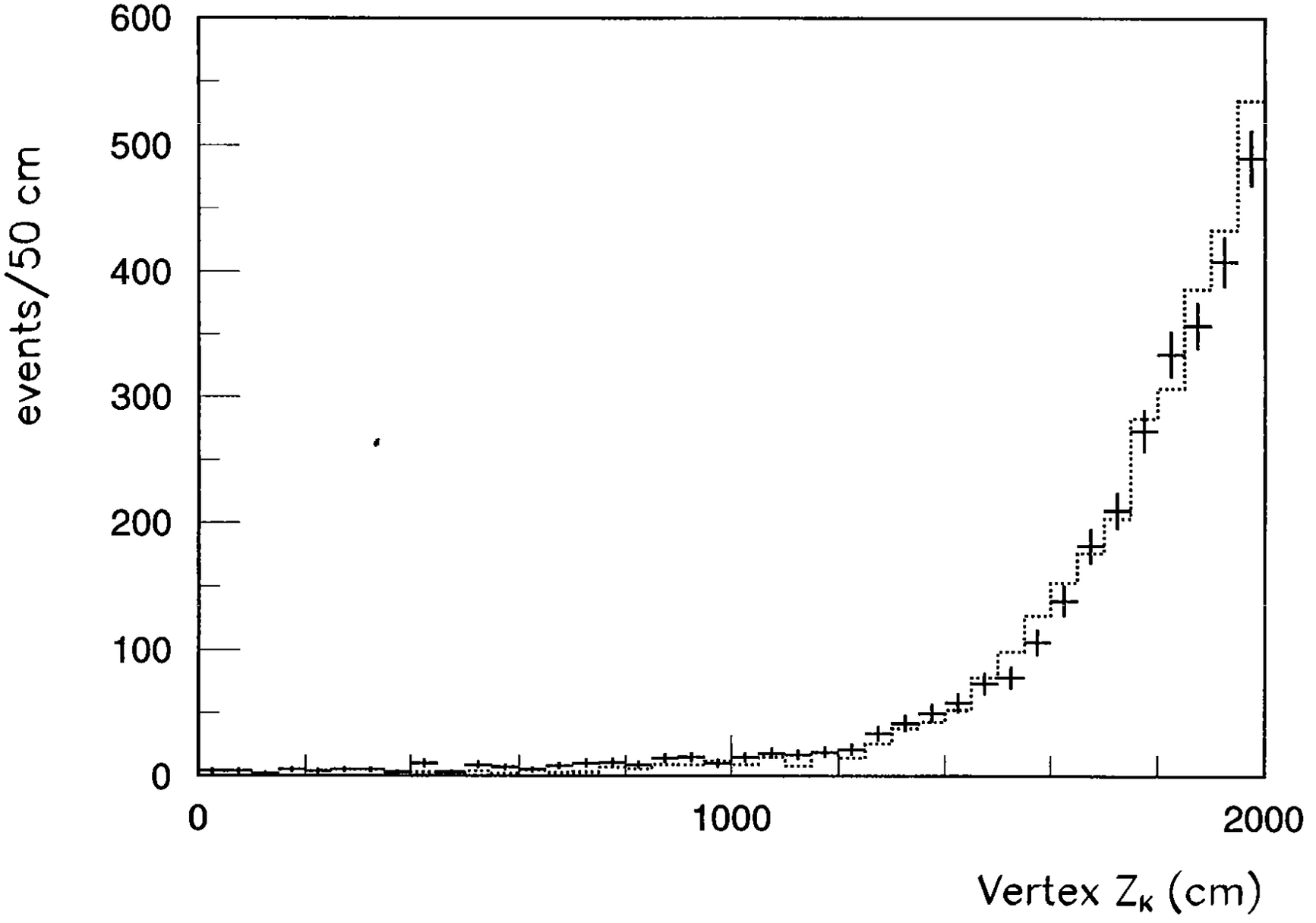

Figure 2

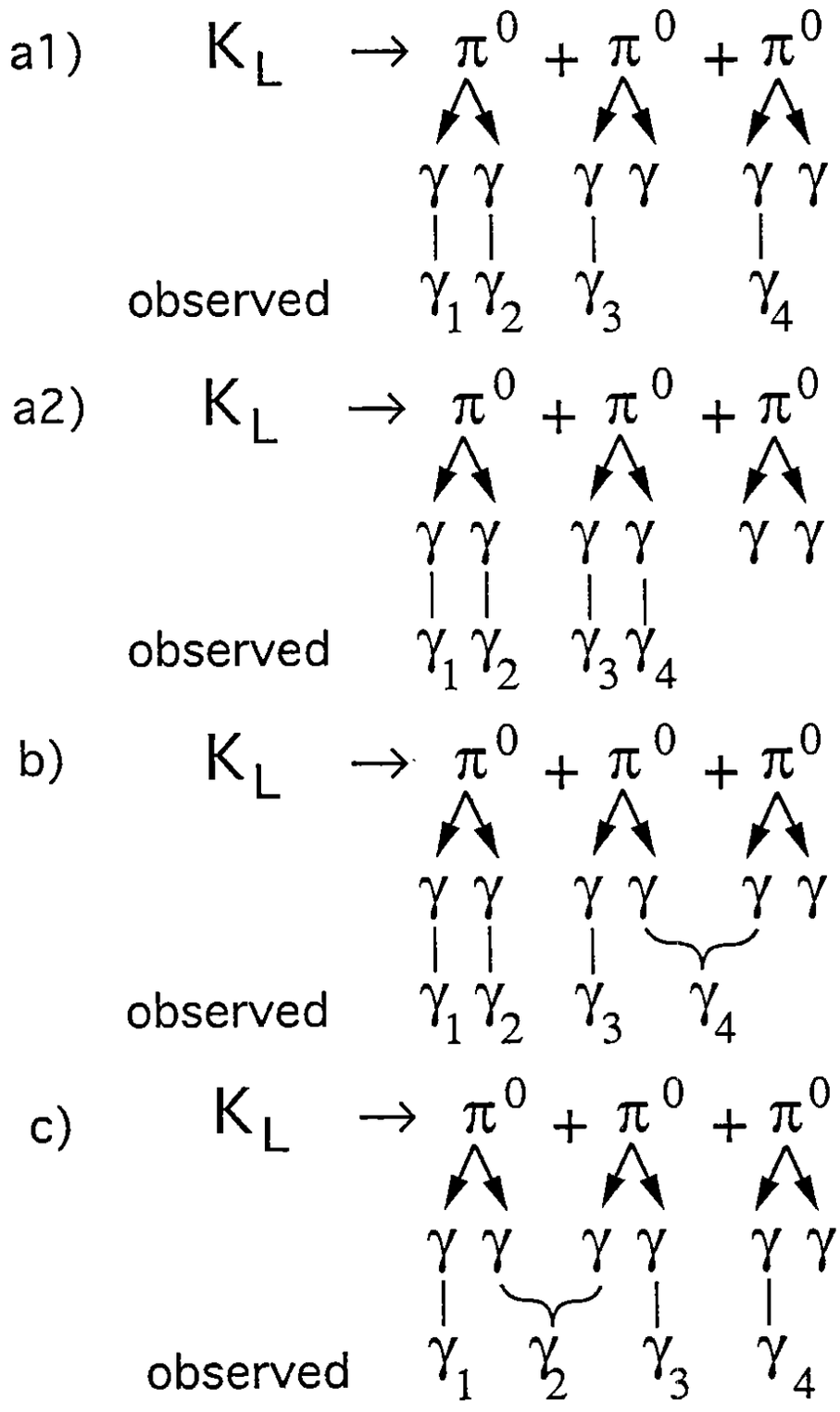
a1)
$K_L \rightarrow \pi^0 + \pi^0 + \pi^0$
observed
$\gamma_1\ \gamma_2\ \gamma_3\ \gamma_4$
a2)
$K_L \rightarrow \pi^0 + \pi^0 + \pi^0$
observed
$\gamma_1\ \gamma_2\ \gamma_3\ \gamma_4$
b)
$K_L \rightarrow \pi^0 + \pi^0 + \pi^0$
observed
$\gamma_1\ \gamma_2\ \gamma_3\ \gamma_4$
c)
$K_L \rightarrow \pi^0 + \pi^0 + \pi^0$
observed
$\gamma_1\ \gamma_2\ \gamma_3\ \gamma_4$

Figure 3

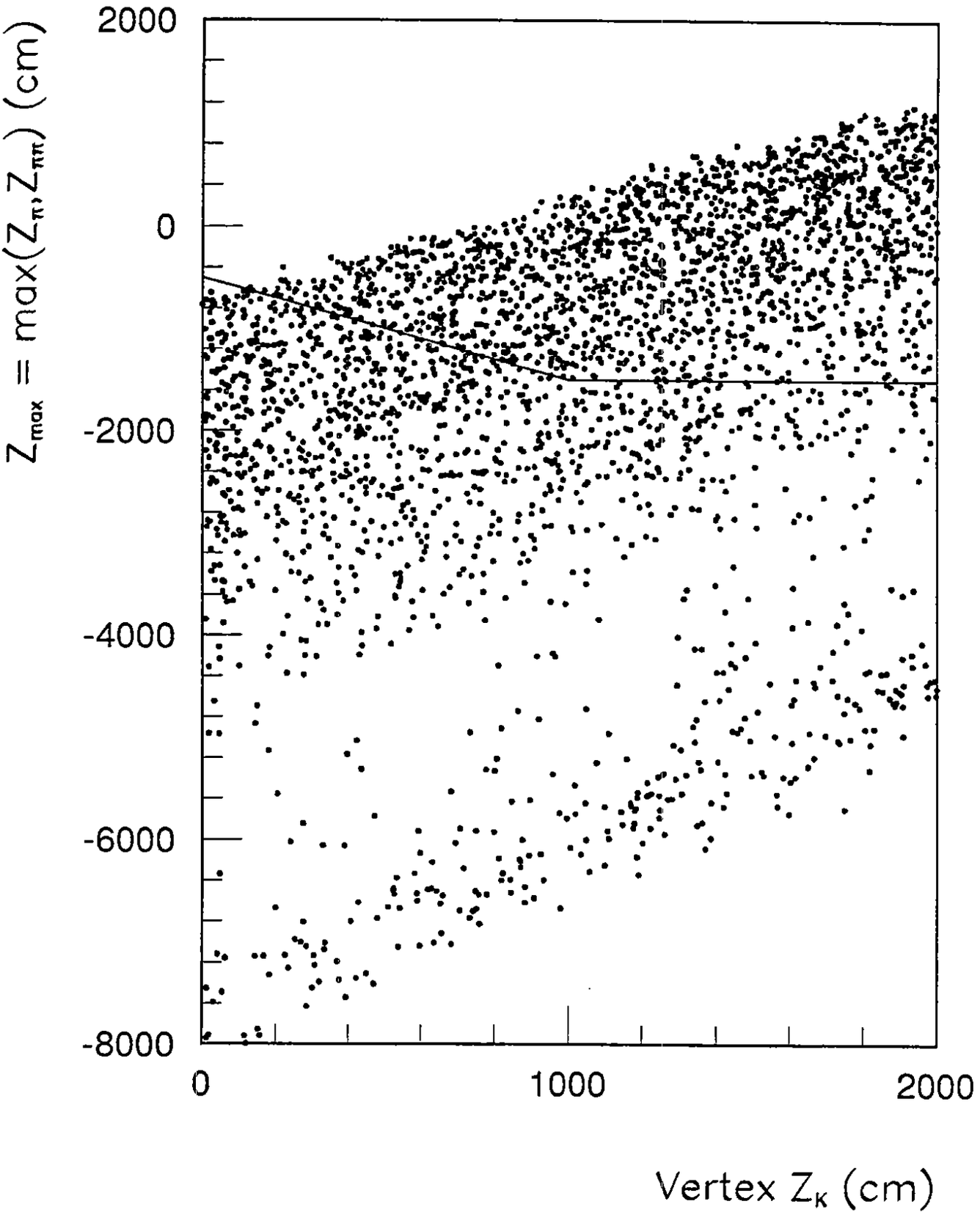
2000
0
-2000
-4000
-6000
-8000
0
1000
2000
$Z_{max} \equiv max(Z_\pi, Z_{\pi\pi})$ (cm)
Vertex Z_K (cm)

Figure 4.a

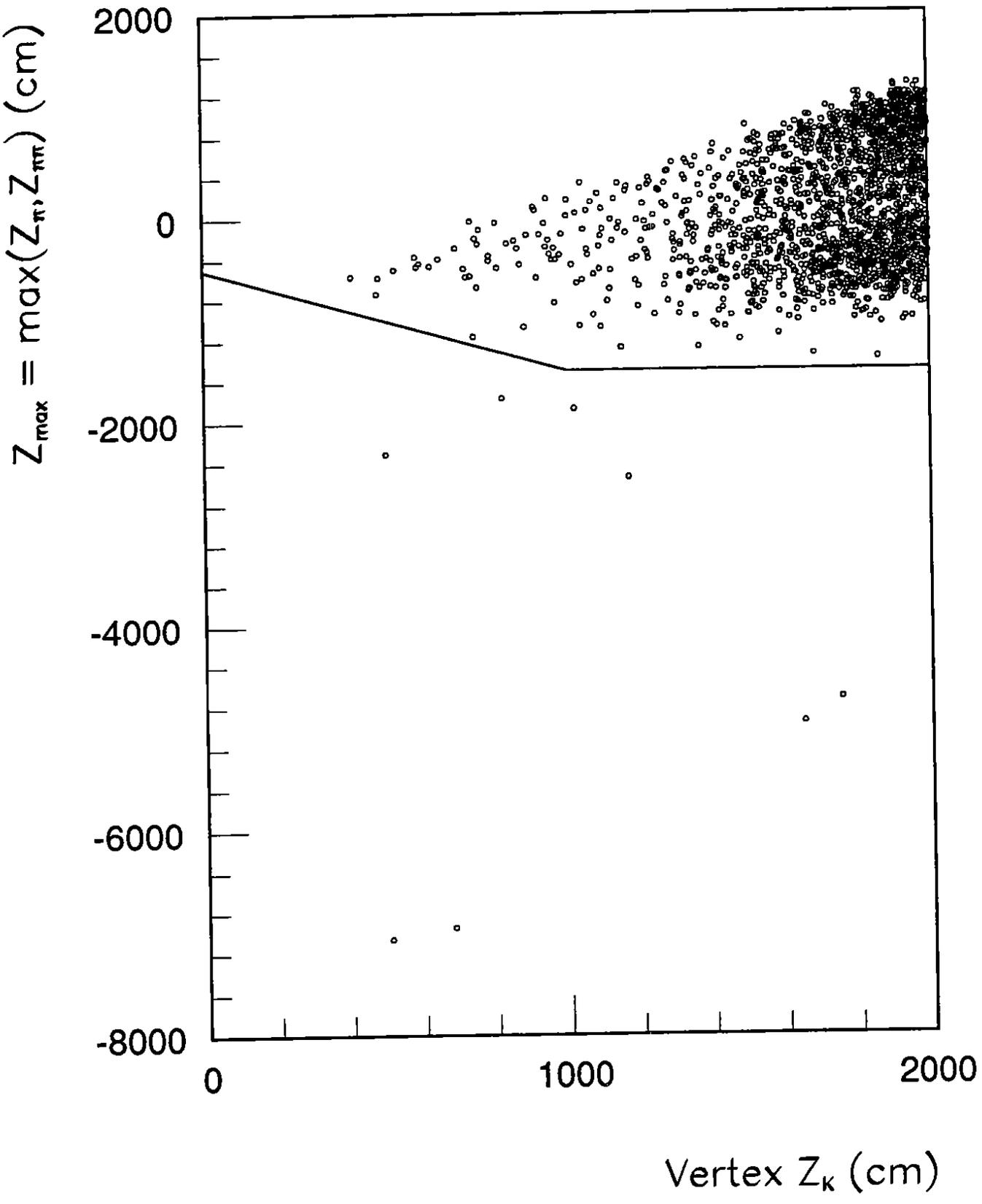
2000
0
-2000
-4000
-6000
-8000
0
1000
2000
$Z_{max} = max(Z_\pi, Z_{\pi\pi})$ (cm)
Vertex Z_K (cm)

Figure 4.b

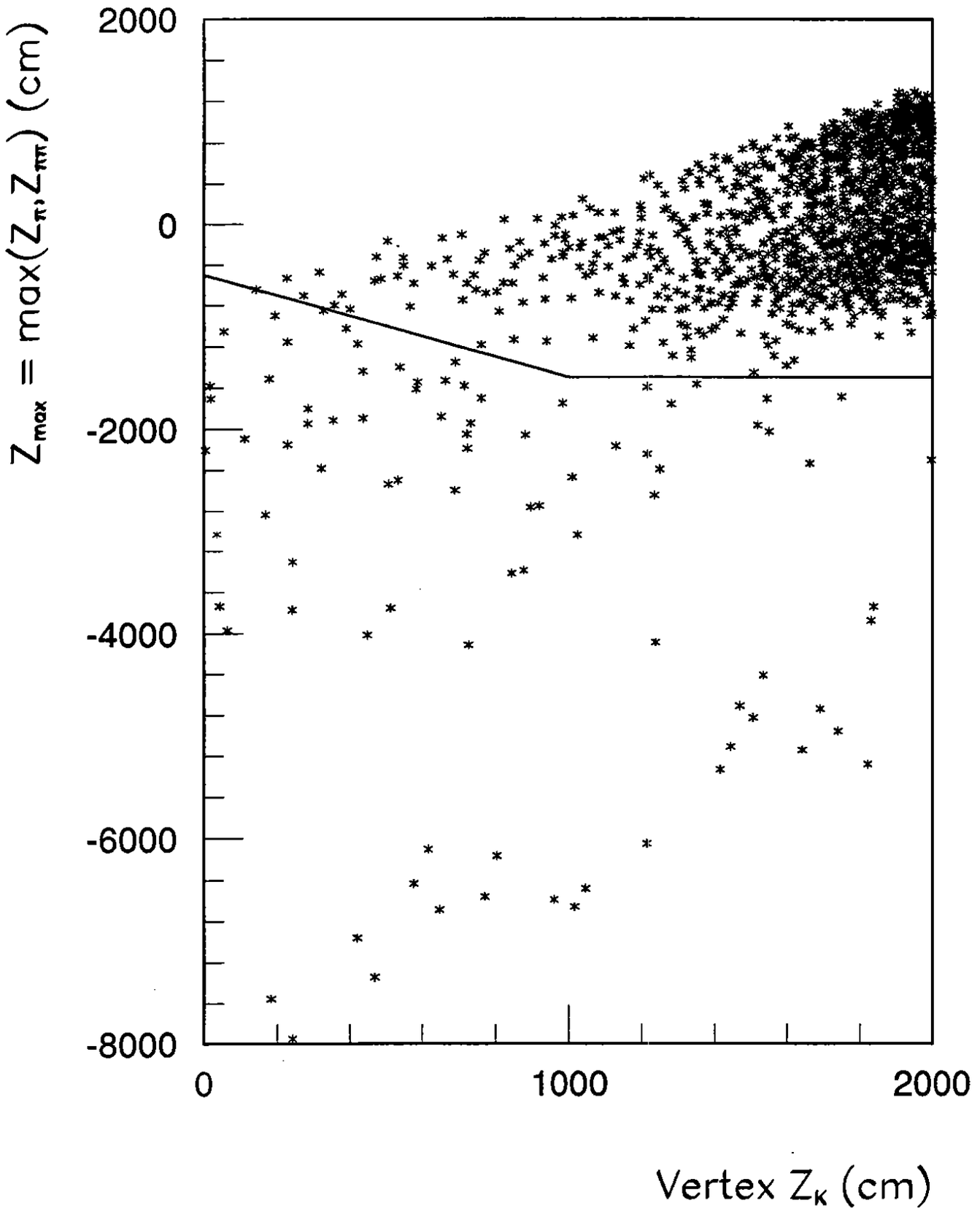
2000
0
-2000
-4000
-6000
-8000
0
1000
2000
$Z_{max} = max(Z_\pi, Z_{\pi\pi})$ (cm)
Vertex Z_K (cm)

Figure 4.c

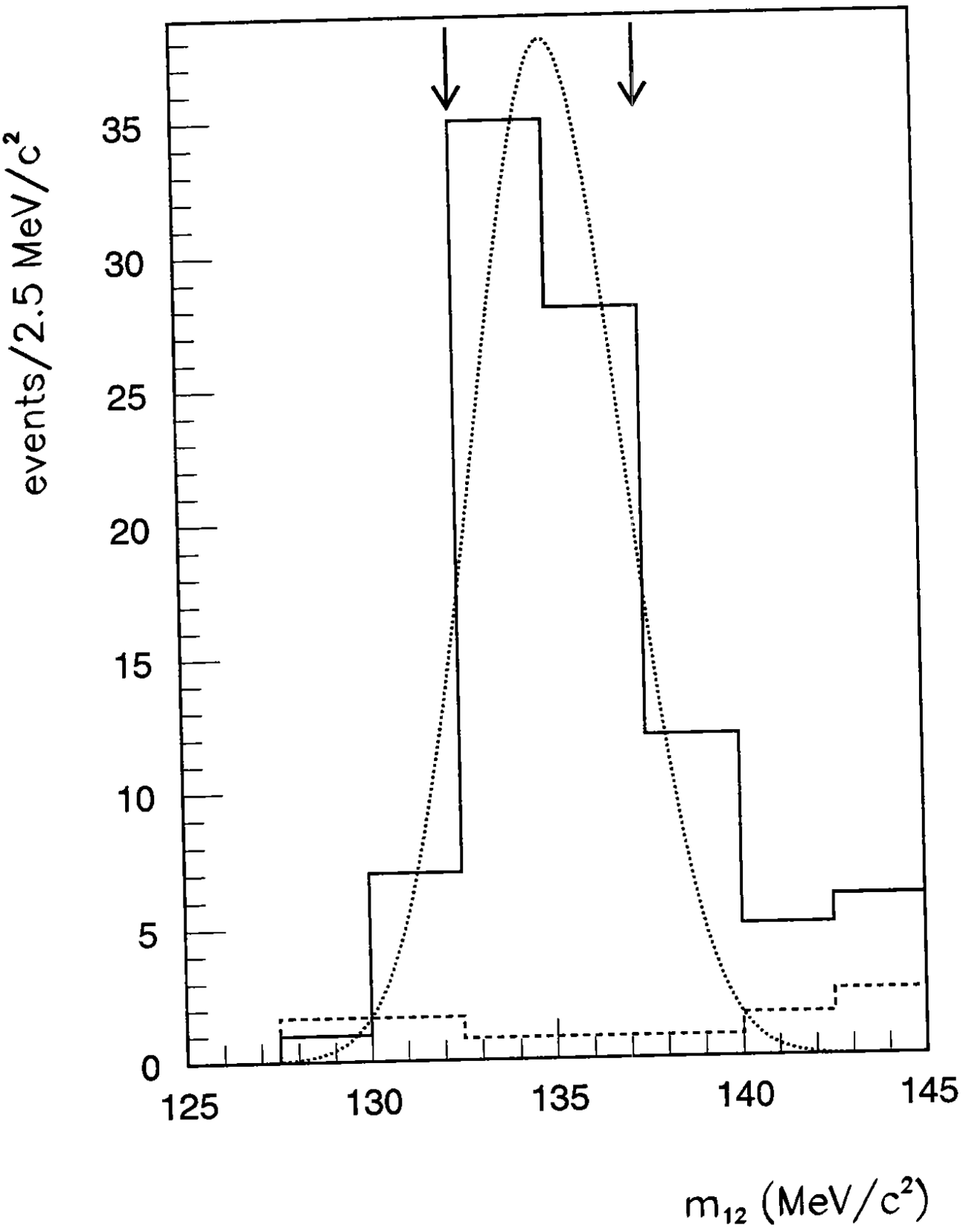
events/2.5 MeV/c²
35
30
25
20
15
10
5
0
125
130
135
140
145
m₁₂ (MeV/c²)

Figure 5

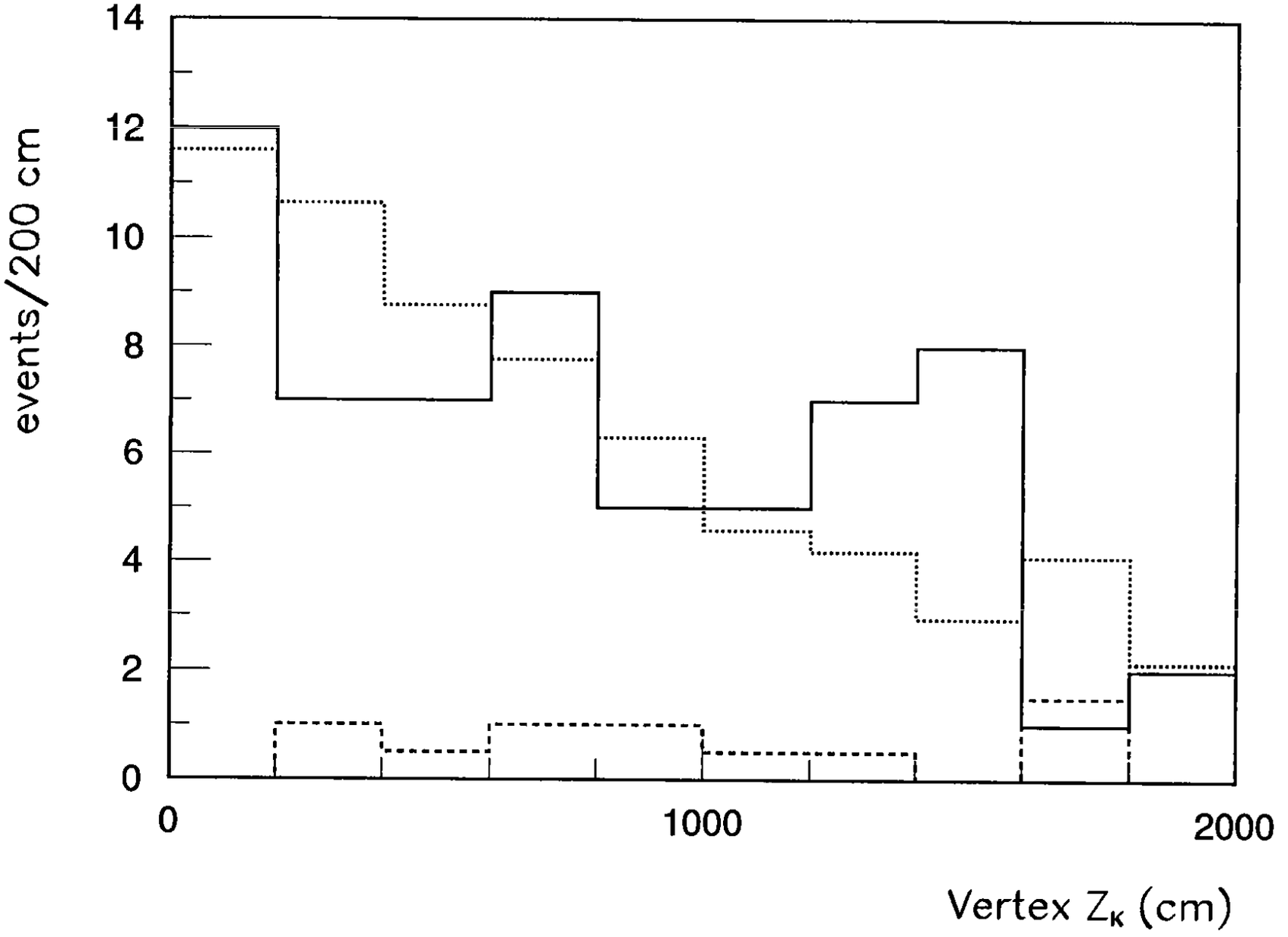

Figure 6

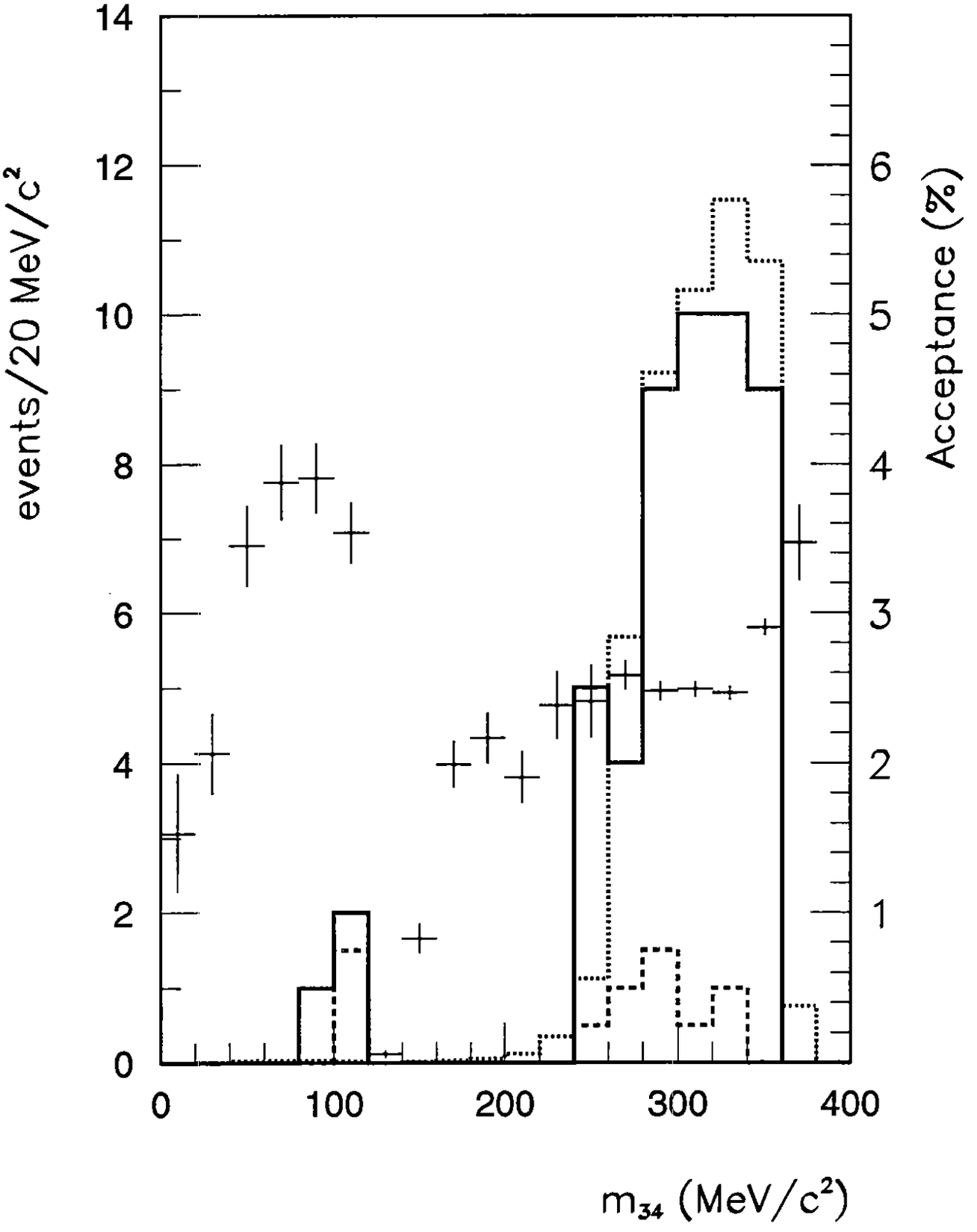
events/20 MeV/c²
Acceptance (%)
m₃₄ (MeV/c²)
0
2
4
6
8
10
12
14
1
2
3
4
5
6
0
100
200
300
400

Figure 7.a

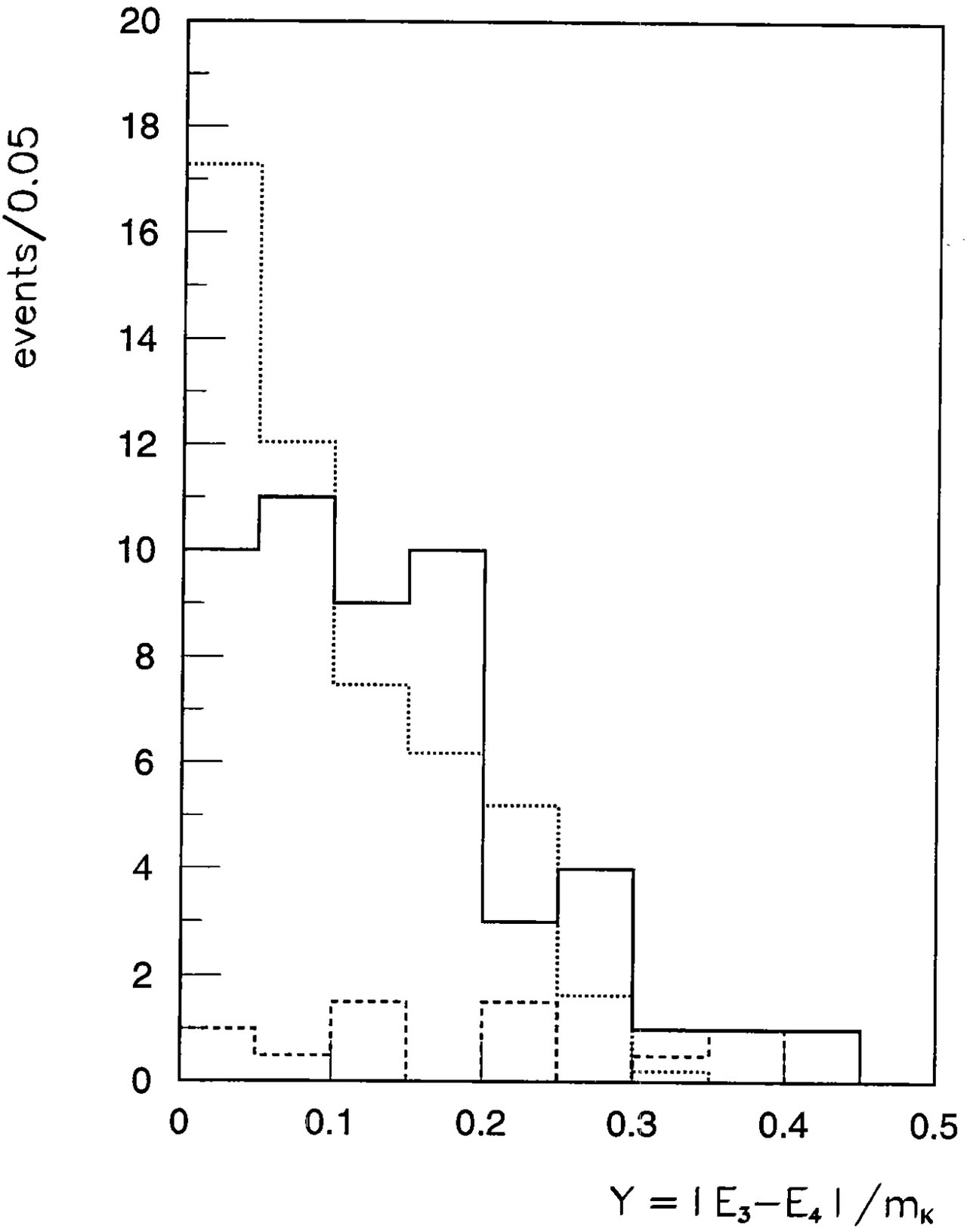

Figure 7.b